Confined Water Body Coverage under Resource Constraints

Ibrahim Salman[a*], Jason Raiti[b*], Nare Karapetyan[c*], Archana Venkatachari[d]
Annie Bourbonnais[d], Jason M. O'Kane[a], and Ioannis Rekleitis[a]

***Abstract*— This paper presents a novel algorithm for monitoring marine environments utilizing a resource-constrained robot. Collecting water quality data from large bodies of water is paramount for monitoring the ecosystem's health, particularly for predicting harmful cyanobacteria blooms. The large spatial dimensions of such bodies of water and the slow varying of water quality parameters make exhaustive, complete coverage impractical and unnecessary. This work explores a new strategy for efficiently measuring water quality quantities with an autonomous surface vehicle (ASV). The method utilizes the medial axis of the water body producing a guideline for the ASV trajectory that visits representative areas of the environment. The proposed method ensures data collection in the narrower parts of the lake, where researchers have historically observed harmful blooms while also visiting open water areas. It also presents an analysis of the Spatio-temporal sensitivity of the target sensor. A comparison with the traditional lawnmower algorithm demonstrates that the conventional BCD-based complete coverage method cannot sample the small coves of a lake. As such, we show that the proposed method captures more diverse regions of the area with a partial coverage technique. Offline analysis of several lakes and reservoirs and results from field deployments at Lake Murray, SC, USA, demonstrate the proposed method's effectiveness.**

I. INTRODUCTION

This paper investigates a novel trajectory planning algorithm of an Autonomous Surface Vehicles (ASV) for monitoring Harmful Cyanobacteria Blooms (HCBs) in fresh surface waters, such as lakes and reservoirs — see Fig. 1, where our ASV [1] collects data at Lake Murray, SC, USA. In order to establish a baseline for the conditions of a water body, data needs to be collected, however, the size of the environment together with the slow rate of change of these measurements makes a grid-based dense sampling unrealistic and unnecessary.

Recent research has demonstrated that ASVs have significant potential for surveying, exploring, and monitoring marine environments [2], [3]. Research is being conducted into Harmful Algal Bloom (HABs) in an effort to better predict and understand them, and there is evidence that global warming is increasing their rate of occurrence [4]. However, previous algal bloom studies note that human monitoring of such HAB events [5] is an extremely time consuming and resource intensive task.

Fig. 1: Autonomous Surface Vehicle collecting bathymetric and water quality data at Lake Murray, SC, USA.

HCBs occur in fresh waters such as lakes, while algal blooms (HABs) occur in salt and brackish waters. They are the result of many different organisms, such as toxic and noxious phytoplankton, macroalgae and benthic algae, and cyanobacteria. In freshwater environments, such as lakes, blooms are mainly caused by benthic algae and cyanobacteria, thus often called Harmful Cyanobacteria Blooms (HCBs). Since 2010 there have been more than 500 reports in the USA of HABs/HCBs[1].

Since the seventies [6], scientists have been trying to monitor, understand and predict algal blooms, a topic that has stayed an active area of research. Remote sensing from satellite images was utilized to observe lakes, albeit in low resolution. The environmental drivers that initiate, maintain, and influence the growth and spread of HCBs are still not fully understood, which impedes their predictability and management. Traditional science relies on manual sampling of the water in distinct locations. This process is labor intensive, time consuming, often exposes scientists to unsafe conditions (contact with toxic algae), and is limited both spatially and temporarily. However, manual sampling/data-collection is the standard approach and provides an excellent starting point and a base of comparison. Within the robotics community, research applicable to this task includes algorithms for coverage of a known environment [7]–[9] or adaptive sampling [2], [10], [11]. For water quality monitoring, it is important to cover large surfaces of water, however, dense patterns generate trajectories that are prohibitively long. Historical data have shown that HCBs

*The first three authors contributed equally to the paper.
[a]Computer Science & Engineering Department, University of South Carolina, USA, ijsalman@email.sc.edu, {jokane, yiannisr}@cse.sc.edu.
[b]Florida State University, jzraiti@gmail.com
[c]University of Maryland, College Park, knare@umd.edu
[d]School of Earth, Ocean, and the Environment, University of South Carolina, USA, {abourbonnais,avenkatachari}@seoe.sc.edu
The authors would like to acknowledge the generous support of the National Science Foundation grants (NSF 1849291, 1923004, 2050896)

[1]https://www.ewg.org/interactive-maps/algal_blooms/map/

develop near the shore and not in the deeper parts of the lake. Furthermore, the quantities of interest do not change rapidly across the surface of the lake. Therefore, the traditional grid sampling pattern (also termed boustrophedon, lawnmower, or seed-spreader algorithms) is prohibitively slow and does not contribute additional information. In contrary, sampling based approaches assume prior knowledge about the environment, based on which they aim to maximize information gain.

This paper presents a novel approach for systematic covering of an aquatic environment, based on utilizing the skeleton [12] (also called medial axis [13] or Generalized Voronoi Graph [14]) of the target area to guide the ASV's trajectory.The skeleton —that is, the set points in free space that are equidistant to multiple distinct points on the obstacle boundary— provides a well established one dimensional retraction of a two dimensional shape [15] used for shape segmentation and object recognition. Consequently, the skeleton traverses through the entire shape and generates a first order representation. In order to spread the coverage trajectory as wide as possible, the medial axis (skeleton) between the original skeleton and the boundaries of free space is used. The resulting trajectory passes through free space, ensuring that the areas closer to shore are visited more.

The main motivation of the proposed approach is the observation that phenomena of interest more often than not occur near shore and in particular start inside small coves which are protected from strong winds and currents. In addition, from a navigation perspective, near-shore operations are increasingly challenging in contrast to operations away from the shores. In other words, in the middle of the lake, there is minimal variation of the water quality values, and a simple lawnmower pattern can be applied. Experimental results from Lake Murray, SC, USA validate our approach, while the algorithm has been used to extract large trajectories of the major lakes in South Carolina to test the scalability of the approach.

II. Related Work

The area coverage path planning problem has been extensively studied in robotics [16], [17]. Depending on the goal or constraints of the coverage operation, different variations have been presented such as coverage under limited resources, complete coverage, information driven coverage or sampling based coverage.

a) Complete Coverage: One of the widely used approaches of Complete Coverage is based on the boustrophedon area decomposition approach, which splits the area of interest into obstacle-free cells and then moves the robot in a lawnmower motion pattern to cover each cell [18]. Several works use this type of motion as the method of choice in solving the coverage problems as a main strategy [19] or as a prior strategy to improve coverage quality [20]. Other approaches were also used for decomposing areas, such as Morse [21] or grid-based [22], [23] decomposition.

Polynomial time algorithms were proposed for solving single robot coverage using a boustrophedon decomposition based approach [24], [25]. In contrast to the original algorithm, in these approaches, the problem is represented as a Chinese postman problem (CPP), which ensures an efficient coverage order of cells.

When considering the coverage problem for robots with turning constraints, the presented methods that use the boustrophedon coverage pattern may not be the most efficient — that is, they will either spend excess time on covering areas out of the region of interest or fail to perform complete coverage on turns because of the rotation constraints. The Dubins vehicle is a common robot model in coverage problems, and Savla *et al*. [26] consider a control-theoretic solution. Lewis *et al*. [9] proposed an algorithm for a single robot with Dubins constraints utilizing a TSP formulation.

The problem of reducing traversal time by the motion constraints was also addressed by Huang [27] and Yao [28]. In these works, motion constraints are used in the environmental decomposition with the objective of reducing the amount of rotation required by the robot. Similarly, to minimize the number of turns with multiple robots, Vandermeulen *et al*. introduced a rank partitioning heuristic that used a multiple travelling salesman (m-TSP) formulation [29].

b) Information-driven Coverage: In many applications, performing complete coverage is infeasible. On the other hand, when prior information is available about the area, and the aim is to maximize the utilization of that prior knowledge, then information driven or sampling based methods are applied [30], [31]. Using this approach, Manjanna et al. [32] were able to create a map of a coral reef area with half the distance travelled and power used than a lawnmower-style complete coverage algorithm would have required. Roznere *et al*. [3] presented preliminary work on utilizing an ASV for HCB monitoring utilizing pre-programmed and information driven trajectories.

c) Skeleton, Medial Axis, center of maximal disks, Generalized Voronoi Graphs: all these terms define the same concept [33], [34] with small variations: the locus of points equidistant from some boundary. The linear skeleton approach [12] operates on a polygon by retracting each edge inwards uniformly, also termed the brushfire transform, until the retracted edges meet. The center of maximal disks describes the same concept, where a maximal disk is a circle inscribed in a shape which is not properly contained in another inscribed circle. The set of all the maximal disk centers defines the same representation. Finally, the most common term, medial axis [13], is the set of all points inside the area of interest with more than one closest point to the boundary of the area.

Generalized Voronoi Graphs (GVGs) were introduced by Choset and Burdick [14] and have been used to guide exploration of indoor spaces, navigating without exact localization [35], and reducing localization error [36]–[38]. GVGs focus on the control laws to guide a robot to stay equidistant from two or more obstacles while navigating in open space.

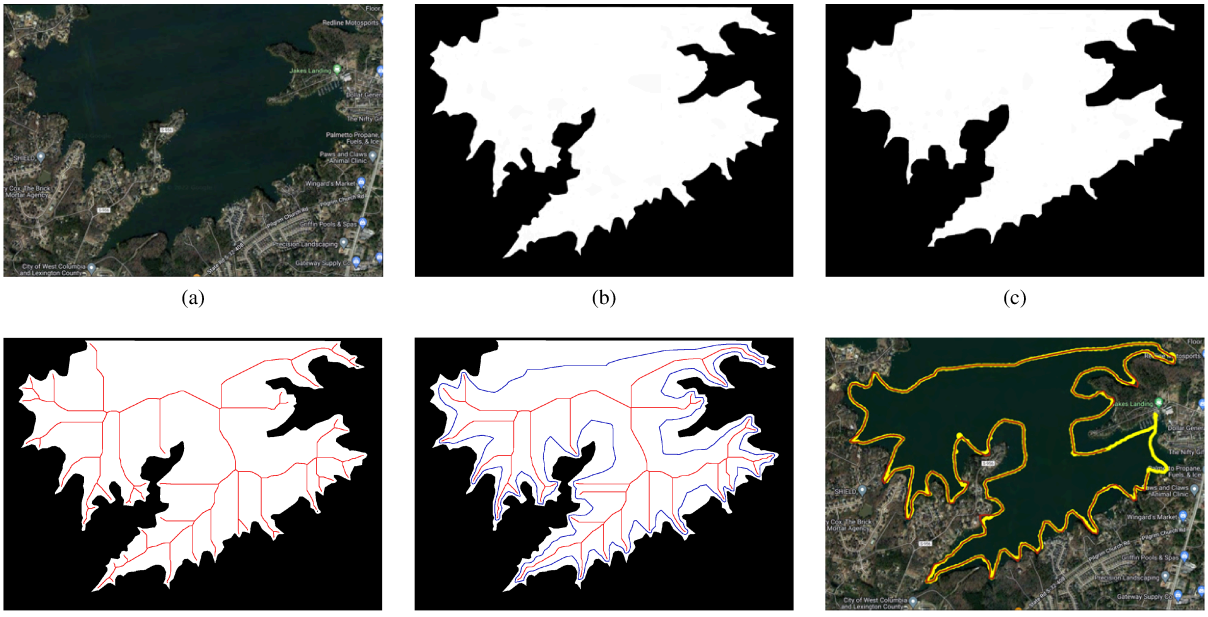

Fig. 2: The proposed approach in images, Lake Murray, SC, USA: (a) The target environment (Satellite). (b) The binary map identifying obstacles and free space. (c) The free space map, obstacles dilated for safety. (d) The skeleton of free space (in red). (e) The skeleton (in red) and the second skeleton between the skeleton and the obstacles (in blue). Both skeletons, trimmed. (f) The generated waypoints for the coverage path together with the GPS points of the executed trajectory.

III. Proposed Approach

The first step of the approach is to select the area of interest on an online map; see, for example Fig. 2(a) for a satellite image from Google Maps. Utilizing the default view and removing the labels results in a clear distinction of the water body from the landmass. An image is captured with the top left and bottom right coordinates in longitude and latitude recorded; the image then is transformed into black and white (white for free space – water, and black for obstacles); see Fig. 2(b). Each pixel in this image has a fixed size in meters as extracted from the recorded latitude-longitude coordinates.

In order to produce safe trajectories, the environment is dilated and eroded using a safety distance (in our case, ten meters) which is translated to a fixed number of pixels; see Fig. 2(c) for the safe environment of Fig. 2(b). Inspection of the satellite map often reveals man-made obstacles that do not appear in the default map. Edits to the black and white obstacle map ensure that such objects are recorded. It is worth noting that the proposed approach is designed for operations in a known environment, as such, expert knowledge, sometimes from on site observations, should be recorded in the map representing the environment.

The morphology of free space is captured by extracting the skeleton of free space; see Fig. 2(d). Several different variants of the skeleton algorithm exist, after experimentation, the Lee *et al.* [39] skeleton algorithm was selected as it resulted in a smaller number of extraneous edges. The next step is to trim the resulting skeleton using the following criteria: edges that barely entered a cove were removed together with smaller edges. Finally, each terminating edge was trimmed a safe distance from the obstacles.

The proposed algorithm utilizes the trimmed skeleton from the previous step in order to produce a cyclic path traversing the perimeter of the skeleton. The key idea is to construct the medial axis (skeleton) between the original skeleton and the dilated environment. The medial axis constructed by two branches of the original skeleton results in dead ends of edges finishing in the middle of the environment, and as such are avoided. Figure 2(e) presents the trimmed skeleton (in red) and the medial axis (in blue) between the trimmed skeleton and the environment. As can be seen, the skeleton guides the path inside the coves while the medial axis generates a path that circumscribes the skeleton, terminating next to the starting point. More formally, for a given point p and set T, define the closest distance from point p to a set of points T as $D^T(p) = \min_{p_t \in T}(d(p, p_t))$, in which d is the Euclidean distance, i.e. the L_2 norm. The medial axis M then is defined as the set of all points in free space P_{free} that are equidistant to the obstacle space O and the original skeleton S, so that: $M = \{p \in P_{free} \mid D^O(p) = D^S(p)\}$.

The produced path traverses through the points that are equidistant to the skeleton and the obstacle boundaries. Every cove (concave area of free space) traverse is divided into three areas from the obstacle to the path, between the two paths (where the original skeleton is located) and then from the other path to the obstacle. Every point of free space is positioned at most at a distance d_max from the path, which is the distance from the path to the nearest obstacle. While traversing the skeleton will trace the same area, the maximum

distance to the path is twice the distance from the proposed approach, and the ASV traverses the same path twice.

Figure 2(f) presents the planned GPS waypoints plotted on top of the satellite image (red) and the resulting GPS trace from the actual deployment in that environment (yellow). There are small deviations where waves pushed the ASV off-course, and it corrected on the way to the next waypoint. The starting and ending points were planned to start outside a no-wake zone with heavy boat traffic, and for safety, the start and end of the experiment were under manual operation.

The resulting path is heavily biased towards the boundaries of the environment as expected. An obvious comparison will be to a shore following algorithm. However, such an approach has two drawbacks: a fixed distance to shore fails to accommodate for the varying width of the coves, as such sampling inside the coves would not be uniform. In addition, in more open areas, the proposed algorithm uniformly divides the free space to travel equidistant from the obstacles and the original skeleton.

IV. Experimental Results

A. Experimental Platform

The vehicle utilized is the Jetyak [1], an ASV developed at the University of South Carolina; see Fig. 1 for the ASV operating at Lake Murray, SC, USA. The ASV is based on a modified Mokai Es-Kape[2] boat. The stock vessel uses an internal combustion engine and reaches speeds up to $22.5\,\mathrm{km/h}$, with a deployment time of over eight hours. The ES-Kape's factory pulse width modulated controlled servo system allows seamless integration with a Pixhawk[3] flight control system and on-board control through a companion Intel UP computer serving to host Robot Operating System (ROS) [40][4]. The Autonomous Surface Vehicle (ASV) [1] has been equipped with a YSI EXO2 multiparameter sonde [41] to collect water quality samples near the surface (at $0.5\,\mathrm{m}$ depth) utilizing the proposed sampling trajectory. In addition, bathymetry data are collected, and the water quality data are augmented with the depth information along the trajectory of collection.

B. A spatio-temporal analysis of the target sensors

There are two factors influencing the proposed coverage pattern: the spatial variation of the measured quantity and the temporal sensitivity of the sensor. From the EXO2 sonde manual [42] the factory reported response time values T63[5] for the sensors attached, ranging between one and five seconds. It is worth noting that data are collected every two seconds (0.5Hz), which is the fastest rate of the Sonde. Dissolved oxygen has the slowest response time with less than five seconds and then pH with less than three seconds. However, as the variables of interest change slowly, we were able to maintain speeds of $6.4Km/h$ with no adverse effects.

[2] http://www.mokai.com/mokai-es-kape/

[3] https://docs.px4.io/en/flight_controller/mro_pixhawk.html

[4] http://wiki.ros.org/

[5] T63 is the time it takes the sensor to reach 63% of the actual value.

C. Target Environment

The proposed system is expected to be deployed in different water bodies wherever harmful blooms occur. In South Carolina, we have selected two lakes: Lake Murray and Lake Wateree. Lake Murray spans more than $200\,\mathrm{km}^2$, and has a shore length in excess of $700\,\mathrm{km}$, with a length of $66\,\mathrm{km}$ and with a maximum depth of $57\,\mathrm{m}$. Lake Wateree covers an area of $49\,\mathrm{km}^2$, with a shore length of $291\,\mathrm{km}$ and a maximum depth of $19.5\,\mathrm{m}$. Both are man-made impoundment lakes used for municipal water supply and recreation. They are subject to extensive nutrient loading and experience reoccurring poorly resolved HCBs that are dominated by the toxin producing cyanobacteria Microcystis aeruginosa in Lake Murray and the benthic cyanobacterium Lyngbya wollei in Lake Wateree [43], [44].

D. Coverage comparison with complete coverage

In this comparison, the length of the trajectory from the proposed approach was used as a guideline to choose the footprint of the boustrophedon decomposition based (BCD) algorithm in order to get approximate similar length trajectories. Figure 3(a) presents a BCD path with a relative small footprint. In order to ensure a safe trajectory the target environment is heavily dilated. Figure 3(b) presents the BCD path with a large footprint. Even with a large footprint, the BCD algorithm resulted in a longer trajectory. The two paths, as presented in Fig. 3 (b,c), were utilized to extract statistics on the quality of coverage.

The two paths were used for comparing the proximity of all free space to the coverage path. Figure 4 shows a heat map where blue indicates close proximity traversing through green, yellow, and finally red for the maximum distance. It is worth noting that for the areas close to shore, especially inside all the coves of the environment, the proposed algorithm results in close proximity coverage. In addition, the proposed algorithm resulted in shortened maximum distances compared to the BCD. Quantitative, Table I presents a comparison of the mean and max distance in meters of the coverage proximity of the two approaches.

The preliminary results show a clear advantage over the boustrophedon decomposition based (BCD) method (Fig. 3(b)) when monitoring a surface with many inlets. When the sensor footprint is large, the BCD-based approach sometimes fails to generate non-overlapping and evenly spaced out passes. Also, since the BCD algorithm has to choose one single coverage direction, it lacks the same ability as the skeleton-based approach to have coverage trajectories spread out in different directions throughout the area of interest, thus providing better access to the inlets of the

TABLE I: Comparison of the two motion strategies in terms of proximity of coverage. All values are in meters.

Strategy	Dist.	Mean	max
Boustrophedon [8]	23,174	75.88	603.09
Skeleton based	17,783	79.12	321.36

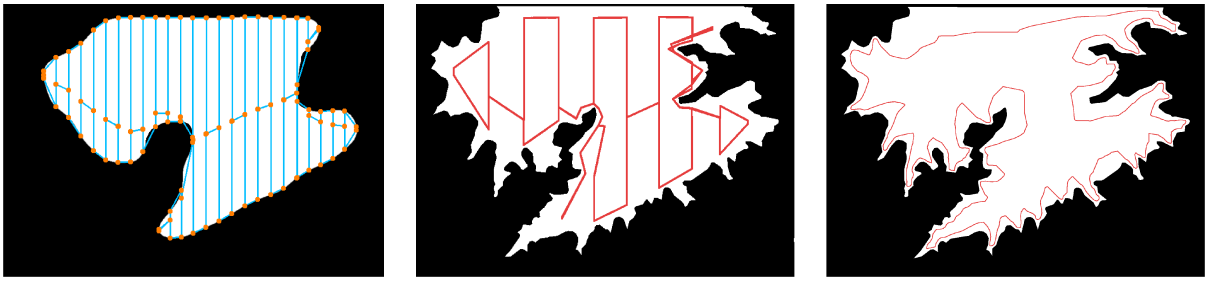

(a) (b) (c)

Fig. 3: (a) Boustrophedon area decomposition based efficient single robot coverage with smaller sensor footprint planned on a heavily dilated obstacle map; (b) $4\times$ larger footprint resulting in a trajectory comparable to the proposed skeleton based algorithm; (c) the proposed algorithm heavily favoring near-shore trajectories.

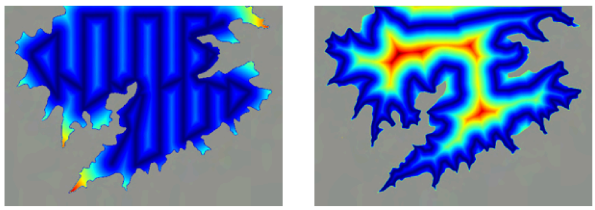

(a) (b)

Fig. 4: Heat-map showing the proximity of each point in open space from the ASV's trajectory for (a) Boustrophedon path, (b) Skeleton-based contour path.

lake. Furthermore, even with a longer trajectory, the BCD average distance of points in free space to the coverage path was approximately the same ($75\,\mathrm{m}$-$79\,\mathrm{m}$); however, the maximum distance of BCD was almost double ($603\,\mathrm{m}$) compared to the max distance resulted from the proposed algorithm ($321\,\mathrm{m}$).

E. Large scale experiments in planning

Different lakes and segments of lakes have been selected, and the proposed algorithm was run on them to verify the scalability of the proposed method. Figure 5(a) presents a trajectory for Lake Murray covering an area of more than $200\,\mathrm{km}^2$, and the resulting trajectory is $548\,\mathrm{Km}$. Figure 5(b) presents a trajectory for a large segment of Lake Murray, the resulting trajectory is $308\,\mathrm{Km}$. The whole area of Lake Wateree is used and Fig. 5(c) shows the trajectory with a length of $144\,\mathrm{Km}$. The above experiments revealed a challenge in the presence of islands. The resulting trajectory consisted of multiple components (going around each island). One solution to this problem is the rearranging of the waypoints so the trajectory bridges out to the separate component and then continues. Future work will address this issue.

F. Field tests at Lake Murray

Several deployments have verified the slow changing values of water quality data, especially in the deeper parts of the lake, away from the shores. Fig. 2(f) presents the GPS track of a deployment, where the ASV traveled through a $17\,\mathrm{Km}$ trajectory, collecting water quality and bathymetric data. Figure 6 presents the water depth along the trajectory and the depth data have been used to evaluate the variance of the water quality data. As can be seen in Fig. 7 pH, temperature, and Dissolved Oxygen (DO) are fairly constant in deeper waters (depths larger than $25\,\mathrm{m}$) while the shallower the water the greater the collected values variance.

V. CONCLUSIONS

In this work, we presented a new algorithm that uses the skeleton of the free space to guide water quality data collection over a confined body of water. Utilizing the skeleton of the free space, the ASV is guided in a circular path visiting all the distinctive areas of the environment (coves and islands) in preference over large open areas. The proposed algorithm has been field tested at Lake Murray in trajectories of over $15\,\mathrm{Km}$ lengths, collecting water quality data. Moreover, compared with a traditional Boustrophedon-based algorithm, the proposed approach reduced the maximum distance of the free space to our trajectory almost by half.

The next task will be to address the issue of disconnected components of produced trajectory in the presence of islands. A trivial solution is to block the passage between islands; however, other alternatives will be investigated [45]. Future work will incorporate obstacle avoidance, particularly dynamic obstacles (boats and jet skis), in combination with mission recovery to enable evasive maneuvering and the continuation of the desired trajectory.

During the summer, when there are more frequent HCB events, the proposed algorithm will be deployed regularly at Lake Murray and Lake Wateree. The collected data, water sampling, and stationary data collection are expected to provide new insights into the development of HCBs.

REFERENCES

[1] J. Moulton, N. Karapetyan, S. Bukhsbaum, C. McKinney, S. Malebary, G. Sophocleous, A. Quattrini Li, and I. Rekleitis, "An autonomous surface vehicle for long term operations," in *MTS/IEEE OCEANS - Charleston*, IEEE, 2018, pp. 1–6.

[2] S. Manjanna *et al.*, "Heterogeneous Multirobot System for Exploration and Strategic Water Sampling," in *IEEE Int. Conf. on Robotics and Automation (ICRA)*, 2018, pp. 4873–4880.

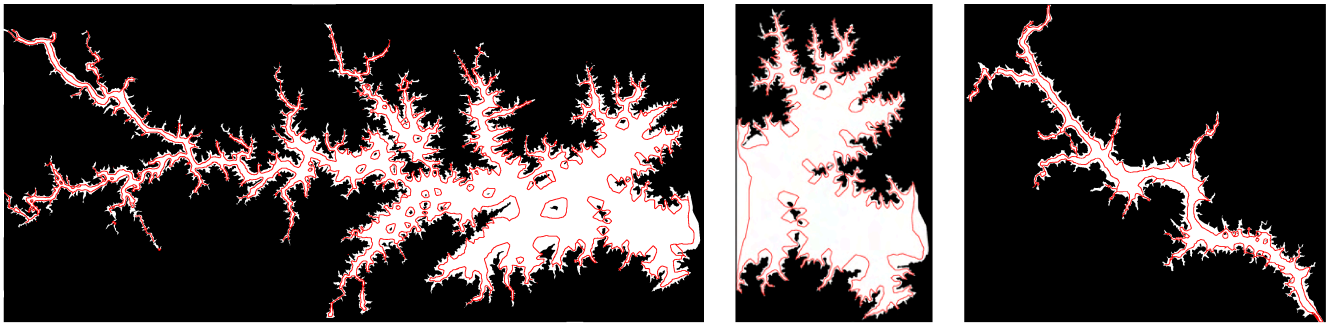

(a) (b) (c)

Fig. 5: Different environments and the resulting skeleton based trajectories (a) and (b) complete and part of Lake Murray;(c) Lake Wateree.

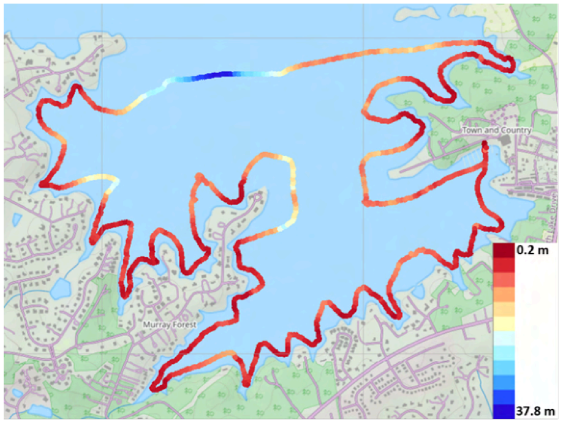

Fig. 6: Depth measurements of Lake Murray along the trajectory of our experiment.

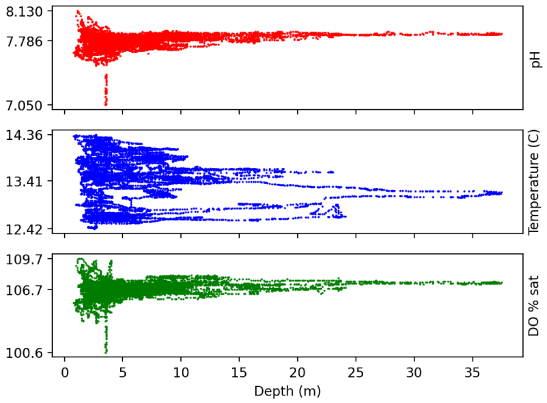

Fig. 7: Data collected utilizing the EXO2 Sonde at Lake Murray along the trajectory of our experiment. pH, Temperature, and Dissolved Oxygen (% sat) are plotted as a function of depth.

[3] M. Roznere *et al.*, "Towards a reliable heterogeneous robotic water quality monitoring system: An experimental analysis," in *Int. Symposium on Experimental Robotics*, Springer, 2020, pp. 139–150.

[4] S. K. Moore *et al.*, "An autonomous platform for near real-time surveillance of harmful algae and their toxins in dynamic coastal shelf environments," *Journal of Marine Science and Engineering*, vol. 9, no. 3, 2021.

[5] E. Zohdi and M. Abbaspour, "Harmful algal blooms (red tide): A review of causes, impacts and approaches to monitoring and prediction," *Int. journal of Environmental Science and Technology*, vol. 16, pp. 1789–1806, Mar. 2019.

[6] R. C. Wrigley and A. J. HORNE, "Remote sensing and lake eutrophication," *Nature*, vol. 250, no. 5463, pp. 213–214, 1974.

[7] N. Karapetyan, K. Benson, C. McKinney, P. Taslakian, and I. Rekleitis, "Efficient multi-robot coverage of a known environment," in *IEEE/RSJ Int. Conf. on Intelligent Robots and Systems (IROS)*, Sep. 2017, pp. 1846–1852.

[8] N. Karapetyan, J. Moulton, J. Lewis, A. Quattrini Li, J. O'Kane, and I. Rekleitis, "Multi-robot Dubins Coverage with Autonomous Surface Vehicles," in *IEEE Int. Conf. on Robotics and Automation*, May 2018, pp. 2373–2379.

[9] J. Lewis, W. Edwards, K. Benson, I. Rekleitis, and J. O'Kane, "Semi-boustrophedon coverage with a dubins vehicle," in *IEEE/RSJ Int. Conf. on Intelligent Robots and Systems (IROS)*, Sep. 2017, pp. 5630–5637.

[10] P. Stankiewicz, Y. Tan, and M. Kobilarov, "Adaptive sampling with an autonomous underwater vehicle in static marine environments," *Journal of Field Robotics*, vol. 38, no. 4, pp. 572–597, 2021.

[11] S. Manjanna, J. Hansen, A. Quattrini Li, I. Rekleitis, and G. Dudek, "Collaborative sampling using heterogeneous marine robots driven by visual cues," in *Canadian Conf. on Computer and Robot Vision (CRV)*, May 2017, pp. 87–94.

[12] O. Aichholzer, F. Aurenhammer, D. Alberts, and B. Gärtner, "A novel type of skeleton for polygons," in *J. UCS The Journal of Universal Computer Science*, Springer, 1996, pp. 752–761.

[13] H. Blum, "A transformation for extracting new descriptors of shape," *Models for Perception of Speech and Visual Forms, 1967*, pp. 362–380, 1967.

[14] H. Choset and J. Burdick, "Sensor based planning, part i: The generalized voronoi graph," in *Int. Conf. on Robotics & Automation (ICRA)*, 1995, pp. 1649–1655.

[15] K. Siddiqi, S. Bouix, A. Tannenbaum, and S. W. Zucker, "Hamilton-jacobi skeletons," *Int. Journal of Computer Vision*, vol. 48, no. 3, pp. 215–231, 2002.

[16] E. Galceran and M. Carreras, "A survey on coverage path planning for robotics," *Robotics and Autonomous systems*, vol. 61, no. 12, pp. 1258–1276, 2013.

[17] H. Choset, "Coverage for robotics–a survey of recent results," *Annals of mathematics and artificial intelligence*, vol. 31, no. 1, pp. 113–126, 2001.

[18] ——, "Coverage of known spaces: The boustrophedon cellular decomposition," *Autonomous Robots*, vol. 9, no. 3, pp. 247–253, 2000.

[19] R. Bähnemann, N. Lawrance, J. J. Chung, M. Pantic, R. Siegwart, and J. Nieto, "Revisiting boustrophedon coverage path planning as a generalized traveling salesman problem," in *Field and Service Robotics*, 2021, pp. 277–290.

[20] A. Khan, I. Noreen, H. Ryu, N. L. Doh, and Z. Habib, "Online complete coverage path planning using two-way proximity search," *Intelligent Service Robotics*, vol. 10, no. 3, pp. 229–240, 2017.

[21] E. U. Acar and H. Choset, "Sensor-based coverage of unknown environments: Incremental construction of morse decompositions," *The Int. Journal of Robotics Research*, vol. 21, no. 4, pp. 345–366, 2002.

[22] Y. Gabriely and E. Rimon, "Spanning-tree based coverage of continuous areas by a mobile robot," *Annals of mathematics and artificial intelligence*, vol. 31, no. 1, pp. 77–98, 2001.

[23] A. Kleiner *et al.*, "A solution to room-by-room coverage for autonomous cleaning robots," in *IEEE/RSJ Int. Conf. on Intelligent Robots and Systems (IROS)*, 2017, pp. 5346–5352.

[24] R. Mannadiar and I. Rekleitis, "Optimal coverage of a known arbitrary environment," in *IEEE Int. Conf. on robotics and automation*, 2010, pp. 5525–5530.

[25] A. Xu, C. Viriyasuthee, and I. Rekleitis, "Efficient complete coverage of a known arbitrary environment with applications to aerial operations," *Autonomous Robots*, vol. 36, no. 4, pp. 365–381, 2014.

[26] K. Savla, F. Bullo, and E. Frazzoli, "The coverage problem for loitering dubins vehicles," in *IEEE Conf. on Decision and Control*, 2007, pp. 1398–1403.

[27] W. H. Huang, "Optimal line-sweep-based decompositions for coverage algorithms," in *IEEE Int. Conf. on Robotics and Automation (ICRA)*, 2001, pp. 27–32.

[28] Z. Yao, "Finding efficient robot path for the complete coverage of a known space," in *IEEE/RSJ Int. Conf. on Intelligent Robots and Systems*, 2006, pp. 3369–3374.

[29] I. Vandermeulen, R. Gros, and A. Kolling, "Turn-minimizing multirobot coverage," in *Int. Conf. on Robotics and Automation*, 2019, pp. 1014–1020.

[30] G. A. Hollinger and G. S. Sukhatme, "Sampling-based robotic information gathering algorithms," *The Int. Journal of Robotics Research*, vol. 33, no. 9, pp. 1271–1287, 2014.

[31] A. Singh *et al.*, "Mobile robot sensing for environmental applications," in *Field and service robotics*, 2008, pp. 125–135.

[32] S. Manjanna, N. Kakodkar, M. Meghjani, and G. Dudek, "Efficient terrain driven coral coverage using gaussian processes for mosaic synthesis," in *Conf. on Comp. and Robot Vision*, 2016, pp. 448–455.

[33] J. E. Goodman and J. O'Rourke, Eds., *Handbook of Discrete and Computational Geometry, Second Edition*. Chapman and Hall/CRC, 2004.

[34] K. Siddiqi and S. Pizer, *Medial representations: mathematics, algorithms and applications*. Springer Science & Business Media, 2008, vol. 37.

[35] K. Nagatani, H. Choset, and S. Thrun, "Towards exact localization without explicit localization with the generalized voronoi graph," in *Int. Conf. on Robotics and Automation (ICRA)*, vol. 1, May 1998, pp. 342–348.

[36] B. Lisien, D. Morales, D. Silver, G. Kantor, I. Rekleitis, and H. Choset, "The hierarchical atlas," *IEEE Trans. on Robotics*, vol. 21, no. 3, pp. 473–481, 2005.

[37] Q. Zhang, D. Whitney, F. Shkurti, and I. Rekleitis, "Ear-based exploration on hybrid metric/topological maps," in *IEEE/RSJ Int. Conf. on Intelligent Robots and Systems (IROS)*, Sep. 2014, pp. 3081–3088.

[38] M. Rezanejad, B. Samari, I. Rekleitis, K. Siddiqi, and G. Dudek, "Robust environment mapping using flux skeletons," in *IEEE/RSJ Int. Conf. on Intelligent Robots and Systems*, 2015, pp. 5700–5705.

[39] T.-C. Lee, R. L. Kashyap, and C.-N. Chu, "Building skeleton models via 3-d medial surface axis thinning algorithms," *CVGIP: Graphical Models and Image Processing*, vol. 56, no. 6, pp. 462–478, 1994.

[40] J. M. O'Kane, *A Gentle Introduction to ROS*. Independently published, Oct. 2013, Available at `http://www.cse.sc.edu/~jokane/agitr/`.

[41] YSI a xylem brand, *Exo2 multiparameter water quality sonde with 7 sensor ports*, `https://www.ysi.com/exo2`, Feb. 2021.

[42] *EXO User Manual, advanced water quality monitoring platform, ITEM# 603789REF, REVISION J*, YSI a xylem brand, 2021.

[43] M. L. Smith, D. C. Westerman, S. P. Putnam, S. D. Richardson, and J. L. Ferry, "Emerging lyngbya wollei toxins: A new high resolution mass spectrometry method to elucidate a potential environmental threat," *Harmful algae*, vol. 90, p. 101 700, 2019.

[44] K. M. Clyburn, "Nutrient limitation of phytoplankton in lake wateree, south carolina: Implications for future water quality management," M.S. thesis, University of South Carolina, 2019.

[45] I. Salman, J. M. O'Kane, and I. Rekleitis, "Uniform coverage of large water bodies with islands under limited resources," in *Robotics for Climate Change (RCC) Workshop at ICRA*, 2022.